Published in final edited form as:
Mol Cell. 2009 June 26; 34(6): 686–695. doi:10.1016/j.molcel.2009.04.032.

Glutamine-Specific N-Terminal Amidase, a Component of the N-End Rule Pathway

Haiqing Wang[1,2,3], **Konstantin I. Piatkov**[1,2], **Christopher S. Brower**[1], and **Alexander Varshavsky**[1,*]

[1]Division of Biology, California Institute of Technology, Pasadena, CA 91125, USA

SUMMARY

Deamidation of N-terminal Gln by Nt^Q-amidase, a previously undescribed N-terminal amidohydrolase, is a part of the N-end rule pathway of protein degradation. We detected the activity of Nt^Q-amidase, termed Ntaq1, in mouse tissues, purified Ntaq1 from bovine brains, identified its gene, and began analyzing this enzyme. Ntaq1 is highly conserved among animals, plants and some fungi, but its sequence is dissimilar to sequences of other amidases. An earlier mutant in the Drosophila *Cg8253* gene that we show here to encode Nt^Q-amidase has defective long-term memory. Other studies identified protein ligands of the uncharacterized human C8orf32 protein that we show here to be the Ntaq1 Nt^Q-amidase. Remarkably, "high-throughput" studies have recently solved the crystal structure of C8orf32 (Ntaq1). Our site-directed mutagenesis of Ntaq1 and its crystal structure indicate that the active site and catalytic mechanism of Nt^Q-amidase are similar to those of transglutaminases.

Keywords

amidohydrolase; proteolysis; ubiquitin; arginylation; tungus

INTRODUCTION

The N-end rule relates the *in vivo* half-life of a protein to the identity of its N-terminal residue (reviewed by (Mogk et al., 2007; Tasaki and Kwon, 2007; Varshavsky, 1996, 2008a; Varshavsky, 2008b). Degradation signals (degrons) that can be targeted by the N-end rule pathway are of two "topologically" distinct kinds: N-terminal degrons, called N-degrons, and internal (non-N-terminal) degrons (Ravid and Hochstrasser, 2008; Varshavsky, 1996; Wang et al., 2008). The main determinant of an N-degron is a destabilizing N-terminal residue of a substrate protein (Figure 1A). The other determinants of N-degron are a substrate's internal Lys residue (the site of formation of a poly-Ub chain) and a nearby unstructured region (Bachmair and Varshavsky, 1989; Prakash et al., 2009; Suzuki and Varshavsky, 1999). An N-

*Corresponding author: Alexander Varshavsky, Division of Biology, California Institute of Technology, Pasadena, CA 91125. Telephone: 626-395-3785. Fax: 626-440-9821. avarsh@caltech.edu.
[2]These authors contributed equally to this work.
[3]Present address: Bristol-Myers Squibb, Research and Development, Department of Metabolism and Pharmacokinetics, Princeton, NJ 08543.

degron is produced from a precursor, called a pre-N-degron, through a protease-mediated cleavage of a substrate that exposes a destabilizing N-terminal residue.

E3 Ub ligases of the N-end rule pathway, called N-recognins, are defined as E3s that can recognize (target) at least some N-degrons (Figure 1A) (Tasaki and Kwon, 2007; Varshavsky, 1996). Some of substrate-binding sites of an N-recognin target N-degrons of specific substrates, while other sites of the same N-recognin target internal (non-N-terminal) degrons of other protein substrates. At least four N-recognins, Ubr1, Ubr2, Ubr4 and Ubr5, mediate the N-end rule pathway in mammals and other multicellular eukaryotes (Figure 1A) (Tasaki and Kwon, 2007; Tasaki et al., 2009). The N-end rule pathway of the yeast Saccharomyces cerevisiae is mediated by a single N-recognin, Ubr1, a 225-kDa sequelog of mammalian Ubr1 and Ubr2 (Hwang et al., 2009; Hwang and Varshavsky, 2008; Xia et al., 2008b). (*A note on terminology*: "sequelog" and "spalog" denote, respectively, a sequence that is similar, to a specified extent, to another sequence, and a 3D structure that is similar, to a specified extent, to another 3D structure. Besides their usefulness as separate terms for sequence and spatial similarities, the rigor-conferring advantage of "sequelog" and "spalog" is their *evolutionary neutrality*, in contrast to interpretation-laden terms such as "homolog", "ortholog" and "paralog" (Varshavsky, 2004).)

The functions of the N-end rule pathway (Figure 1A) include selective degradation of misfolded proteins; the sensing of nitric oxide (NO), oxygen, heme, and short peptides; the fidelity of chromosome segregation; the control of peptide import; regulation of signaling by transmembrane receptors, through the NO/O_2-controlled degradation of specific RGS proteins that regulate G proteins; regulation of DNA repair, apoptosis, meiosis, spermatogenesis, neurogenesis, and cardiovascular development; the functioning of specific organs, in particular the brain and the pancreas; and regulation of leaf senescence, seed germination, and other processes in plants ((Eisele and Wolf, 2008; Holman et al., 2009; Hu et al., 2005; Hu et al., 2008; Hwang et al., 2009; Hwang and Varshavsky, 2008; Rao et al., 2001; Tasaki and Kwon, 2007; Varshavsky, 2008a; Xia et al., 2008a; Zenker et al., 2005), and refs. therein).

The N-end rule has a hierarchic structure (Figure 1A). N-terminal Asn and Gln are tertiary destabilizing residues in that they function through their enzymatic deamidation, to yield the secondary destabilizing N-terminal residues Asp and Glu (Baker and Varshavsky, 1995; Kwon et al., 2000). Destabilizing activity of N-terminal Asp and Glu requires their conjugation to Arg, one of the primary destabilizing residues, by the *ATE1*-encoded Arg-tRNA-protein transferase (R-transferase) (Hu et al., 2005; Hu et al., 2008; Kwon et al., 2002). In mammals and other eukaryotes that produce NO, the set of arginylated residues contains not only Asp and Glu but also N-terminal Cys, which is arginylated after its oxidation to Cys-sulfinate or Cys-sulfonate, in reactions that require NO, oxygen (O_2) or their derivatives (Figure 1A) (Hu et al., 2005; Tasaki and Kwon, 2007).

In S. cerevisiae, the deamidation branch of the N-end rule pathway is mediated by the Nta1 $Nt^{N,Q}$-amidase, which can deamidate either Asn or Gln at the N-termini of polypeptide substrates (Baker and Varshavsky, 1995). In mammals and other multicellular eukaryotes, N-terminal Asn and Gln are deamidated by N-terminal amidases (Nt-amidases) of two kinds (Figure 1A). One of them, the previously characterized Ntan1 Nt^{N}-amidase, is specific for N-terminal Asn (Grigoryev et al., 1996). In part through analyses of *Ntan1*$^{-/-}$ mice, which could not deamidate N-terminal Asn (Kwon et al., 2000), it has been inferred that there also exists a Gln-specific Nt^{Q}-amidase.

In the present work, we detected the activity of Nt^{Q}-amidase, termed Ntaq1, in mouse tissues, purified Ntaq1 from bovine brains, identified its gene, and began studies of this previously undescribed enzyme (Figure 1A). The sequence of mouse Ntaq1 (Nt^{Q}-amidase) is highly

conserved among animals, plants and some fungi, but is dissimilar to sequences of other amidases, including the N-terminal amidases Ntan1 (Nt^N-amidase) and Nta1 ($Nt^{N,Q}$-amidase). A *tungus* mutant in the previously uncharacterized Drosophila melanogaster *Cg8253* gene was found to have defective long-term memory (Dubnau et al., 2003). We show here that this Drosophila gene encodes the counterpart of mouse Ntaq1. In addition, previous proteomic studies identified ~15 putative protein ligands of an uncharacterized human protein encoded by *C8orf32* ((Lim et al., 2006) and refs. therein). We show here that C8orf32 is the human Ntaq1 Nt^Q-amidase. Remarkably, "high-throughput" crystallographic studies of human proteins have recently solved the crystal structure of C8orf32 (Ntaq1) (Bitto et al., 2008). In conjunction with its crystal structure, our site-directed mutagenesis of Ntaq1 indicates that the active site and catalytic mechanism of Nt^Q-amidase are similar to those of transglutaminases. Thus, the discovery and study of Nt^Q-amidase as a component of the N-end rule pathway (Figure 1A) were "instantly" complemented by a crystal structure of this enzyme, a set of its putative protein ligands, and evidence for its role in memory processes.

RESULTS

The S. cerevisiae Nta1 $Nt^{N,Q}$-amidase (Baker and Varshavsky, 1995) (Figure S1) belongs to the nitrilase superfamily, defined through sequelogies (sequence similarities) and spalogies (spatial similarities) (Varshavsky, 2004) among its members. Mammalian Ntan1 Nt^N-amidases, which can deamidate N-terminal Asn but not N-terminal Gln (Grigoryev et al., 1996), are not sequelogous to yeast Nta1. Initially, we attempted a bioinformatics-based identification of a putative Nt^Q-amidase, termed Ntaq1. Several (weak) sequelogs of mouse Ntan1 or S. cerevisiae Nta1 were identified in the mouse genome, but none of those proteins, when expressed in *nta1*Δ S. cerevisiae, were able to restore the Gln-specific branch of the N-end rule pathway in that mutant (data not shown). The resulting impasse led to a direct-isolation approach (Figure 1B, C).

Detection of Mouse Nt^Q-Amidase and Purification of Bovine Nt^Q-Amidase

Reporters for the Nt^Q-amidase assay (Figure 1B and Figure S2A) comprised the E. coli dihydrofolate reductase (DHFR) moiety fused to a C-terminal peptide (denoted as "bt") that was biotinylated in vivo, and also the N-terminal His_{10}-Ub moiety followed by a sequence derived from the N-terminal sequence of α-lactalbumin (Hu et al., 2008). The resulting set of reporters, His_{10}-Ub-**X**-(LTKCEV)-DHFRbt (**X** = Q; E; N; EQ; MQ; GQ; REQ) is denoted as His_{10}-Ub-**X**-DHFRbt. A purified His_{10}-Ub-**X**-DHFRbt was immobilized, via its C-terminal biotin moiety, on neutravidin beads, and thereafter treated with purified USP2cc deubiquitylating enzyme to remove N-terminal His_{10}-Ub, followed by incubation with a cell extract. The resulting samples were washed and incubated with purified R-transferase and radiolabeled Arg, followed by SDS-PAGE and autoradiography of a reporter (Figure 1B, Figure 2A–C and Figure S2).

This assay (Figure 1B) detected varying levels of Nt^Q-amidase activity in all mouse tissues examined (Figure 2A, B and Figure S2). Control assays included incubations of immobilized X-DHFRbt reporters with buffer alone, before the addition of R-transferase (Figure 2B). The Nt^Q-amidase activity was detected by comparing the arginylation of Glu-DHFRbt, a substrate of R-transferase (Figure 1A), to the arginylation of Gln-DHFRbt, which can be arginylated only after its N-terminal deamidation (Figure 1B and Figure 2A, B). Yet another control involved pre-heating of brain extracts at 95°C for 5 min. Glu-DHFRbt could be arginylated by the (subsequently added) R-transferase irrespective of whether a brain extract was heated or unheated before incubation with this reporter. In contrast, the same test with Gln-DHFRbt resulted in a negligible arginylation if a heated brain extract was used (data not shown), implying that deamidation of Gln-DHFRbt was an enzymatic reaction. The non-reporter bands

of ^{14}C-labeled (arginylated) proteins were endogenous proteins that cofractionated with neutravidin beads (Figure 2A and Figure S2B). Some of these proteins might be physiological substrates of R-transferase.

Having detected Nt^{Q}-amidase (Ntaq1), we developed a procedure for its purification from calf brains that included ammonium sulfate precipitation of proteins from a brain extract, followed by ion exchange, hydrophobic and gel filtration chromatography (Figure 1C, Figure 2C and Figure S3A, B). In the last step, a gel filtration on a Superose-12 column, the Ntaq1 Nt^{Q}-amidase activity migrated as a symmetric peak at ~26 kDa (vis-a-vis globular proteins as M_r standards) (Figure 2C). Silver staining of SDS-PAGE-fractionated proteins from peak activity fractions showed two nearly comigrating major bands, the lower band being more abundant in the peak activity fraction (Figure 2C, D). The two proteins were separately excised from the gel and partially sequenced, using in-gel digestion with trypsin and mass spectrometry (MS) (Figure 2D). The upper band was identified as the bovine counterpart of the human heme-binding protein HEBP2. The lower band was identified as the 207-residue bovine counterpart of human C8orf32 (FLJ10204), a previously inferred 205-residue (24-kDa) protein of unknown function (Figure 2D).

Identification and Characterization of the Mouse Ntaq1 Nt^{Q}-Amidase

Mouse *Hebp2* cDNA and *Wdyhv1* cDNA (Acc. No. NC_000081.5) (the latter is the counterpart of human *C8orf32 (FLJ10204)* cDNA) were subcloned into the plasmid p425Met25. The FLAG-tagged mouse Hebp2^{f} and Wdyhv1^{f} were expressed in an *nta1*Δ mutant of S. cerevisiae that lacked the endogenous Nta1 Nt^{N,Q}-amidase, and cell extracts were examined using the Nt^{Q}-amidase assay described in Figure 1B. Although mouse Hebp2^{f} and Wdyhv1^{f} were expressed in S. cerevisiae at comparable levels, as determined by SDS-PAGE and immunoblotting with anti-FLAG antibody, only extracts from cells that expressed Wdyhv1^{f} exhibited the Nt^{Q}-amidase activity (data not shown). To verify the conclusion that Wdyhv1^{f} was the Ntaq1 Nt^{Q}-amidase (Figure 1A), we examined Wdyhv1^{f} in vivo as well, using *nta1*Δ S. cerevisiae that carried plasmids expressing Ub-X-β-galactosidases (Ub-X-βgals), a set of reporters in which X was a variable residue. Cotranslational deubiquitylation of these Ub fusions produces X-βgal reporter proteins. Their enzymatic activity can be employed to compare metabolic stabilities of these (otherwise identical) reporters bearing different N-terminal residues (Baker and Varshavsky, 1995; Varshavsky, 2005).

As would be expected (Figure 1A), the levels of Asp-βgal and Glu-βgal (their degradation does not require deamidation) were low in all of the tested genetic backgrounds, signifying short in vivo half-lives of these X-βgals, whereas the levels of long-lived Met-βgal were high in the same backgrounds (Figure 3A–D). The levels of Asn-βgal and Gln-βgal were high in *nta1*Δ cells but could be made low by re-introduction of yeast *NTA1* encoding Nt^{N,Q}-amidase (Figure 3A, D). Crucially, the levels of Gln-βgal were high in *nta1*Δ S. cerevisiae but became low in the presence of the mouse Ntaq1^{f} Nt^{Q}-amidase (Figure 3A, B). A “reciprocal” result was obtained with *nta1*Δ cells that expressed the previously characterized mouse Ntan1 Nt^{N}-amidase (Figure 3A, C). Thus, mouse Ntaq1 and Ntan1 are specific for N-terminal Gln and N-terminal Asn, respectively, but not for both of these residues, in contrast to S. cerevisiae Nta1. These in vivo results, in agreement with the in vitro data cited above, confirmed the identification of mouse Ntaq1 as an Nt^{Q}-amidase.

Depletion of Mouse Ntaq1 in Vivo and in Cell Extracts

A plasmid that expressed a mouse Ntaq1-EGFP fusion from the P_{CMV} promoter was transiently transfected into NIH-3T3 cells. The resulting fluorescence patterns (Figure S3C–H) suggested a cytosolic/nuclear location of Ntaq1. One caveat is that Ntaq1-EGFP was overexpressed in comparison to the endogenous Ntaq1 Nt^{Q}-amidase. The endogenous *Ntaq1* gene is expressed,

at varying levels, in most cell types, given the presence of Nt^Q-amidase activity in all mouse tissues examined (Figure 2A–D and S2). In agreement with this conclusion, the data in Allen Brain Atlas (http://www.brain-map.org/) indicate that *Ntaq1* mRNA (denoted as *Cg8253* in the Atlas) is expressed, at varying levels, throughout the mouse brain.

A mouse gene (Acc. No. NC_000081.5), termed *Ntaq1* in the present work, is located on Chromosome 15, is ~17.2 kb long, contains 6 exons, and encodes the 209-residue (24-kDa) Ntaq1 Nt^Q-amidase (Figure 4A). The mouse genome does not contain statistically significant sequelogs of mouse *Ntaq1*, suggesting (but not proving) that *Ntaq1* is the sole source of Nt^Q-amidase at least in mammals. Given the in vitro and in vivo evidence described above (Figure 1–Figure 3), it was expected that a down-regulation of *Ntaq1* in mouse cells would result in a decrease of Nt^Q-amidase activity. To verify this expectation, we carried out RNAi with mouse NIH-3T3 cells that expressed *Ntaq1*-specific pre-microRNA (pre-miRNA), and indeed observed a significant decrease of the in vivo levels of both the Nt^Q-amidase activity and the Ntaq1 protein, in comparison to control cells (Figure S4A, B; see Experimental Procedures and the legend to Figure S4 for details). This decrease could be detected either by carrying out the Nt^Q-amidase activity assay with extracts of RNAi-treated and mock-treated cells (Figure S4A), or by immunoblotting the same extracts with an affinity-purified rabbit anti-Ntaq1 antibody, raised against purified mouse Ntaq1 that was produced in the yeast Pichia pastoris (Figure 2E and Figure S4B).

In a different, in vitro-based approach, we selectively depleted Ntaq1 from cell extracts, using the above affinity-purified anti-Ntaq1 antibody. A depletion of endogenous Ntaq1 from extracts of NIH-3T3 cells with the antibody to Ntaq1 resulted in extracts that did not contain Nt^Q-amidase activity above "nonspecific" (control) backgrounds, whereas the otherwise identical treatment of cell extracts with preimmune serum did not significantly decrease this activity (Figure 5A and Figure S4C–E). In agreement with the absence of (statistically significant) sequelogs of mouse *Ntaq1* in the mouse genome, the effect of *Ntaq1*-specific RNAi on the activity of Nt^Q-amidase and a similar but even stronger effect of depleting Ntaq1 with anti-Ntaq1 antibody (Figure 5A and Figure S4) suggested (but did not prove) that Ntaq1 is the sole Nt^Q-amidase in the mouse.

Substrate Specificity of Ntaq1 Nt^Q-Amidase

The Nt^Q-amidase assay (Figure 1B) was applied to C-terminally His_6-tagged, purified mouse Ntaq1 ($Ntaq1^{H6}$) that was expressed in the yeast P. pastoris (Figure 2E). The results confirmed the Gln-specific Nt^Q-amidase activity of Ntaq1 (Figure 5B), and also indicated that Ntaq1 could be inhibited by thiol-specific reagents such as iodoacetamide or N-ethylmaleimide (data not shown). To address the properties of Ntaq1 in yet another way, **X**-(LTKCEV)-DHFRbt reporters (**X** = Q; N; E; MQ; GQ; EQ) were incubated with purified mouse $Ntaq1^{H6}$, followed by N-terminal sequencing of the resulting proteins by Edman degradation. **Gln**-((LTKCEV)-DHFRbt became **Glu**-(LTKCEV)-DHFRbt after incubation with Ntaq1, whereas **Asn**-(LTKCEV)-DHFRbt, **Glu**-(LTKCEV)-DHFRbt, **Met-Gln**-(LTKCEV)-DHFRbt, **Gly-Gln**-(LTKCEV)-DHFRbt, and **Glu-Gln**-(LTKCEV)-DHFRbt remained unchanged (Figure 3F). These experiments directly demonstrated that Ntaq1 is an Nt^Q-amidase, and also showed that Gln at position 2 was not a substrate of Ntaq1, confirming its high specificity for N-terminal Gln (Figure 5C).

At this stage of the project, we developed an entirely different Nt^Q-amidase assay, which utilized purified Ntaq1 and 7-residue synthetic peptides **XY**-GSGAW (**XY** = QH; QK; QL; QD; QY; QP; KQ; YH; NH; Ac-QH) as reporters (Figure 4B, C). In this "Q-peptide" assay, deamidation of, for example, Gln-HGSGAW was measured by quantifying the production of ammonia (NH_3). It was detected through the presence of NADH-dependent glutamate dehydrogenase (Figure 4B). The consumption of NADH, monitored through a decrease of

A_{340}, was used to measure the formation of ammonia and thus the activity of purified Nt^{Q}-amidase. In agreement with the inferred specificity of Ntaq1 for the unmodified N-terminal Gln of a polypeptide, the Q-peptide assay showed that Ntaq1 could not deamidate acetylated N-terminal Gln, and was also inactive toward non-Gln N-terminal residues (Figure 4C). With the sole exception of proline, all tested second-position residues did not influence the activity of Ntaq1 by more than 2-fold (Figure 4C). In contrast, a Pro at position 2, in the Q**P**GSGAW peptide, virtually abolished deamidation of N-terminal Gln (Figure 4C), a potential clue to stereochemistry and mechanism of Nt^{Q}-amidase.

Three-Dimensional Structure, Mutational Analysis, and Mechanism of Ntaq1 Nt^{Q}-Amidase

Strong sequelogs of the mouse, human and bovine Ntaq1 Nt^{Q}-amidases are present throughout the animal kingdom (including fishes, insects and nematodes), in plants (including Arabidopsis thaliana), and in some fungi, such as the fission yeast Schizosaccharomyces pombe, but not in the budding yeast S. cerevisiae (Figure S5). (S. cerevisiae contains the Nta1 $Nt^{N,Q}$-amidase (Figure S1).) Although Ntaq1 of the present work and the previously characterized Ntan1 (Kwon et al., 2000) catalyze analogous reactions (Figure 1A), there is no statistically significant sequelogy among Ntaq1, Ntan1 and Nta1. This remarkable lack of sequelogy suggests independent origins of these Nt-amidases, presumably late in evolution of the N-end pathway, after the emergence of its arginylation branch (Figure 1A). In contrast to Nt-amidases, there is a sequelogy between eukaryotic Ate1 R-transferases (Figure 1A) and prokaryotic Bpt L-transferases (Graciet et al., 2006), suggesting that beginnings of the N-end rule's arginylation branch predate the emergence of eukaryotes.

While preparing this study for publication we came across a recent entry in the Protein Data Bank (PDB #3C9Q; target name: BC008781) (Bitto et al., 2008). This entry, a part of "high-throughput" crystallographic studies by the Center for Eukaryotic Structural Genomics, described the crystal structure of the otherwise uncharacterized C8orf32 human protein (Figure 6A). As shown by our findings (Figure 2–Figure 5, Figure S2–S4, and discussion above), the mouse Ntaq1 Nt^{Q}-amidase is the counterpart of human C8orf32. Consequently, C8orf32 will now be called Ntaq1. The 1.5 Å structure of human Ntaq1 (C8orf32), solved with a bound peptide-like compound with a well-resolved N-terminal tripeptide Ser-Thr/Val-Ala (Bitto et al., 2008), is a monomeric globular protein of a novel structural fold, with an α-β-α three-layer sandwich architecture (Figure 6A). The residues Cys^{28}, His^{81} and Asp^{97} (they correspond to Cys^{30}, His^{83} and Asp^{99} in mouse Ntaq1) are highly conserved among Ntaq1 proteins of different organisms (Figure S4) and are spatially proximal in the crystal structure of human Ntaq1 (Figure 6C), in a region that resembles an active site, in proximity to the bound peptide-like compound (Bitto et al., 2008).

Guided by Ntaq1 sequence alignments (Figure S5) and the crystal structure of human Ntaq1 (Figure 6A), we used site-directed mutagenesis and expression in the yeast P. pastoris to produce and purify 9 mutants of mouse Ntaq1, in addition to wild-type enzyme (Figure 2E and data not shown). The results of examining these mutants by the Q-peptide assay were in agreement with the inferred significance of Cys^{30} and His^{83} as key residues of the active site (Figure 4D). Specifically, $Ntaq1^{C30A}$ and $Ntaq1^{H83A}$ had no detectable Nt^{Q}-amidase activity, in contrast to wild-type or nearly wild-type levels of activity exhibited by mutants at other evolutionarily conserved positions, such as $Ntaq1^{C23A}$, $Ntaq1^{C28A}$, $Ntaq1^{C-38A}$, $Ntaq1^{E39Q}$, and $Ntaq1^{H170A}$ (Figure 4E). The $Ntaq1^{D81N}$ mutant was impaired but still active (Figure 4D).

An analogous Cys…His…Asp triad of spatially proximal residues mediates the catalysis by cysteine proteases (such as, for example, papain), and by transglutaminases as well. The latter enzymes catalyze an acyl transfer in which the γ-carboxamide group of an internal Gln residue in a polypeptide acts as the acyl donor, usually to the ε-amino group of a Lys residue, resulting in an isopeptide bond that crosslinks two polypeptides or different regions of the same

polypeptide. There is no significant sequelogy between Ntaq1 Nt^Q-amidases (Figure S4) and other proteins, including cysteine proteases or transglutaminases. Remarkably, however, we found (using Entrez-3D and the VAST algorithm) that human Ntaq1 is spalogous (spatially similar) to mouse peptide N-glycanase (PDB 2F4M_A) in the region of the glucanase's "transglutaminase core" domain. Given this result, we carried out a spatial alignment between Ntaq1 (Figure 5A) and Factor XIII transglutaminase (Figure 6B) (Pedersen et al., 1994). The inferred active site region of the human Ntaq1 Nt^Q-amidase was found to be a strikingly strong spalog of the active site of human transglutaminase factor XIII, despite the absence of sequelogy between these enzymes (Figure 6C; compare with Figure 6D).

In the catalysis of crosslinking by transglutaminases, the ε-amino group of a Lys residue attacks a (transiently) enzyme-linked Gln residue of a substrate polypeptide (Pedersen et al., 1994), but an attack by water is possible as well, leading, in such instances, to deamidation of Gln to Glu by a transglutaminase. To examine the "converse" possibility of Nt^Q-amidase exhibiting a transglutaminase activity, we employed a crosslinking assay with biotinylated cadaverin as a source of amino group (Dutton and Singer, 1975), a Gln-DHFR reporter, and purified mouse Ntaq1. No crosslinking of cadaverin to Gln-DHFR by Ntaq1 was observed (data not shown), suggesting (but not proving, given the logic of negative evidence) that Nt^Q-amidase is devoid of transglutaminase activity. This tentative conclusion is also consistent with the absence of sequelogy between Nt^Q-amidases and transglutaminases. Taken together, our results with site-directed mutants of Nt^Q-amidase (Figure 4D), the obvious spalogy (but no sequelogy) between the active sites of Nt^Q-amidase and transglutaminases (Figure 6C, D), and the resulting Cys…His…Asp catalytic triade of Nt^Q-amidase lead us to propose the verifiable conjecture that deamidation of N-terminal Gln by the Ntaq1 Nt^Q-amidase employs a transglutaminase-like catalytic mechanism.

DISCUSSION

Progress in biological research, including "high-throughput" structural studies, has produced a disposition all but improbable a decade ago: the Ntaq1 Nt^Q-amidase, a previously undescribed enzyme, finds itself surrounded by directly relevant genomic, proteomic and even crystallographic evidence. These earlier data have become unified and informed in the present work by the revealed enzymatic identity of Ntaq1, its mechanistic similarity to transglutaminases, and its place in the N-end rule pathway. Before the present study, the *Ntaq1* gene was called *Cg8253* in Drosophila melanogaster, *Wdyhv1* in mice and *C8orf32* in humans (Figure 2D and Figure S5). Some of the vistas opened up by our findings about the Ntaq1 Nt^Q-amidase stem from earlier data, such as, for example, the detection of putative protein ligands of human C8orf32 (Ntaq1) ((Lim et al., 2006) and refs. therein), which remain to be explored.

A mutant, termed *tungus*, in Drosophila *Cg8253* (*Ntaq1*) that encodes the fly counterpart of mouse Nt^Q-amidase, has defective long-term memory ((Dubnau et al., 2003); see also FlyBase FBrf0188553). This finding is consistent with the previously demonstrated major role of the N-end rule pathway in mouse brain development (An et al., 2006), with some of the putative ligands of human C8orf32 (Ntaq1) being relevant to neurodegeneration syndromes (Lim et al., 2006), with regulation of the nematode (C. elegans) counterpart of mouse *Ntaq1* by neuron-specific transcription factors (NCBI>GEO>Series GSE9665), and with an involvement of human C8orf32 (Ntaq1) in regulation of genes containing cAMP-response elements (Tian et al., 2007).

Deamidation of N-terminal Gln by Nt^Q-amidase (Figure 1A) is mutually exclusive with the formation of N-terminal pyroglutamate. The latter reaction is catalyzed by glutaminyl cyclase (Schilling et al., 2008). Nt^Q-amidase is present in the cytosol and the nucleus (Figure S3C–H),

as is the rest of the N-end rule pathway, whereas glutaminyl cyclase is in the secretory compartment, including the endoplasmic reticulum (ER). However, given complexities of traffic between intracellular compartments (including retrotranslocation of proteins from the ER to the cytosol), the extent of in vivo "competition" between Nt^Q-amidase and glutaminyl cyclase, i.e., the extent of overlap between the sets of their physiological substrates, remains to be determined.

Despite their multiplicity and broad range, the discovered functions of the N-end rule pathway (see Introduction) are still the tip of the iceberg. The known physiological substrates of this pathway (Hwang et al., 2009; Varshavsky, 2008a) are the beginning of a longer list that may require new methods for its systematic elucidation. Given their distinct N-terminal residues, Asn versus Gln, the sets of physiological substrates of Nt^N-amidase (Ntan1) and Nt^Q-amidase (Ntaq1) most likely do not overlap. Therefore it is not possible to predict, at present, whether *Ntaq1*$^{-/-}$ mice will be viable as adults, similarly to *Ntan1*$^{-/-}$ mice (Kwon et al., 2000), or whether they will be embryonic lethals, similarly to *Ate1*$^{-/-}$ mice, which lack N-terminal arginylation, a step downstream of N-terminal deamidation (Figure 1A) (Kwon et al., 2002).

The subunit selectivity of processive proteolysis, first discovered in the context of the N-end rule pathway (Johnson et al., 1990), underlies most functions of the Ub system, as it allows protein remodeling through subunit-specific degradation. A cleaved subunit whose C-terminal fragment bears a destabilizing N-terminal residue (Figure 1A) would be a potential substrate for selective proteolytic removal from a protein complex, thus making possible its remodeling (Johnson et al., 1990; Prakash et al., 2009). Because the N-end rule pathway can target either N-degrons or internal (non-N-terminal) degrons (see Introduction), this remodeling can involve not only cleaved but also intact subunits of a protein complex. Previous work indicated that one function of the N-end rule pathway is to operate, in such contexts, as a device that employs its capacity for subunit-specific proteolysis to reset the states of relevant circuits. Examples include the degradation of a separase-produced fragment of a cohesin subunit, a step that has been shown to be required for the high fidelity of chromosome segregation (Rao et al., 2001; Varshavsky, 2008a). Another likely example is the degradation of the yeast Mgt1 DNA alkylguanine transferase (Hwang et al., 2009). Recent studies (Huang et al., 2006) suggested that a circuit-resetting function of the N-end rule pathway may involve the Ntaq1-dependent degradation of a fragment of the USP1 deubiquitylating enzyme, whose substrates include ubiquitylated PCNA, the DNA replication processivity factor. Conditional self-cleavage of human USP1 produces a C-terminal fragment of USP1 that bears N-terminal Gln. This fragment is apparently short-lived in vivo (Huang et al., 2006), and may be an N-end rule substrate targeted for degradation by the Ntaq1 Nt^Q-amidase. A verification of this conjecture should be possible through the use of *Ntaq1*$^{-/-}$ mouse strains. Their construction is under way.

EXPERIMENTAL PROCEDURES

For a detailed description of Experimental Procedures, see Supplemental Data.

Reporter Proteins

In the reporter proteins His_{10}-Ub-**X**LTKCEV-DHFRbt (see the legend to Figure 1B), **X** was a 1-, 2-or 3-residue sequence (**X** = Q; E; N; EQ; MQ; GQ; REQ)

Nt^Q-Amidase Assay with X-DHFR Reporters

This assay was based on coupling the deamidation of N-terminal Gln to the arginylation, by purified R-transferase, of the resulting N-terminal Glu residue (Figure 1A) in the presence of radiolabeled Arg. The assay is outlined in Figure 1B and described in Supplemental Data.

Nt^{Q}-Amidase Assay with Synthetic Peptides

This assay, which employed purified Nt^{Q}-amidase and 7-residue peptides **XZ**-GSGAW (**XZ** = QH; QK; QL; QD; QY; QP; KQ; YH; NH; Ac-QH), measured deamidation-produced ammonia using NADH-dependent glutamate dehydrogenase, as described in Supplemental Data.

Purification of Bovine Ntaq1 Nt^{Q}-Amidase

Nt^{Q}-amidase was purified from calf brains through steps that included ion exchange, hydrophobic and gel filtration chromatography (Figure 1C, Figure 2C, Figure S2 and S3A, B). Mass spectrometry (MS-MS) identified a partially purified bovine Nt^{Q}-amidase as the counterpart of a previously uncharacterized protein encoded by human *C8orf32*. See Supplemental Data for details.

Plasmids for Expression of Mouse Ntaq1 in S. cerevisiae

C-terminally FLAG-tagged mouse Ntaq1 Nt^{Q}-amidase ($Ntaq1^{f}$) and other proteins were expressed in S. cerevisiae from the high-copy vector p425MET25 (Table S1)

Expression of Mouse Ntaq1 in Pichia pastoris

ORFs encoding C-terminally His_6-tagged mouse Ntaq1 Nt^{Q}-amidase ($Ntaq1^{H6}$) and its missense mutants were subcloned into pPICZα-C (Table S1) and expressed in the yeast P. pastoris, followed by purification of overexpressed proteins by Ni-affinity chromatography.

β-Galactosidase Assay

Assays for βgal activity (Baker and Varshavsky, 1995) were performed with extracts from WHQ8 (*nta1*Δ) S. cerevisiae carrying pUB23-X plasmids (X = Met, Asp, Asn, Glu, or Gln) that expressed Ub-X-βgal reporters.

Site-Directed Mutagenesis

Alterations of specific residues in mouse Ntaq1 were carried out using two-step PCR and pPICZα-mNtaq1-mNtaq1 (Table S1).

N-terminal Sequencing of Reporter Proteins

Purified **X**LTKCEV-DHFRbt proteins (**X** = MQ; EQ; GQ; E; Q; N) were incubated with purified mouse Ntaq1 Nt^{Q}-amidase, followed by SDS-PAGE and N-terminal sequencing of test proteins by Edman degradation

Ntaq1-EGFP Reporter

A fusion between mouse Ntaq1 and EGFP was constructed in the pEGFP-N1 vector (Clontech) and examined with NIH-3T3 mouse cells as described in the main text.

Antibody to Mouse Ntaq1 and Depletion of Ntaq1 from Mouse Cells and Cell Extracts

A rabbit antibody to Ntaq1 was produced using mouse $Ntaq1^{H6}$ (see above) purified from P. pastoris. The antibody was affinity-purified using immobilized $Ntaq1^{H6}$, and was thereafter employed (vis-a-vis preimmune serum) to deplete the Ntaq1 Nt^{Q}-amidase from extracts of NIH-3T3 cells (Figure 5A, Figure S4C–E, and Supplemental Data). RNAi procedures for down-regulation of the expression of endogenous Ntaq1 in mouse NIH-3T3 cells using pre-microRNAs (pre-miRNAs) (Figure S4A, B) are described in Supplemental Data.

Supplementary Material

Refer to Web version on PubMed Central for supplementary material.

ACKNOWLEDGMENTS

We thank current and former members of the Varshavsky laboratory for their advice and help, particularly R.-G. (Cory) Hu and Z. Xia for the plasmids pWHQ91 and pH10UE. We are grateful to J. Zhou and E. A. Wall (California Institute of Technology) for assistance with Ntaq1 mass spectrometry and genetic analysis, respectively, and to B. Stanley and A. Stanley (Pennsylvania State University, Hershey, PA) for N-terminal sequencing of reporter proteins. This study was supported by grants to A. V. from the National Institutes of Health (GM31530, GM85371, DK39520) and the American Asthma Foundation.

REFERENCES

An JY, Seo JW, Tasaki T, Lee MJ, Varshavsky A, Kwon YT. Impaired neurogenesis and cardiovascular development in mice lacking the E3 ubiquitin ligases UBR1 and UBR2 of the N-end rule pathway. Proc Natl Acad Sci USA 2006;103:6212–6217. [PubMed: 16606826]

Bachmair A, Varshavsky A. The degradation signal in a short-lived protein. Cell 1989;56:1019–1032. [PubMed: 2538246]

Baker RT, Varshavsky A. Yeast N-terminal amidase: a new enzyme and component of the N-end rule pathway. J Biol Chem 1995;270:12065–12074. [PubMed: 7744855]

Bitto E, Bingman CA, McCoy JG, Wesenberg GE, Phillips GN J. Crystal structure of the uncharacterized human protein C8orf32 with bound peptide. 2008Protein Data Bank, PDB 3CQ9.

Dubnau J, A-S C, Grady L, Barditch J, Gossweiler S, McNeil J, Smith P, Buldoc F, Scott R, Certa U, et al. The staufen/pumilio pathway is involved in Drosophila long-term memory. Curr Biol 2003;13:286–296. [PubMed: 12593794]

Dutton A, Singer SJ. Crosslinking and labeling of membrane proteins by transglutaminase-catalyzed reactions. Proc Natl Acad Sci USA 1975;72:2568–2571. [PubMed: 241075]

Eisele F, Wolf DH. Degradation of misfolded proteins in the cytoplasm by the ubiquitin ligase Ubr1. FEBS Lett 2008;582:4143–4146. [PubMed: 19041308]

Graciet E, Hu RG, Piatkov K, Rhee JH, Schwarz EM, Varshavsky A. Aminoacyl-transferases and the N-end rule pathway of prokaryotic/eukaryotic specificity in a human pathogen. Proc Natl Acad Sci USA 2006;103:3078–3083. [PubMed: 16492767]

Grigoryev S, Stewart AE, Kwon YT, Arfin SM, Bradshaw RA, Jenkins NA, Copeland NG, Varshavsky A. A mouse amidase specific for N-terminal asparagine. The gene, the enzyme, and their function in the N-end rule pathway. J Biol Chem 1996;271:28521–28532. [PubMed: 8910481]

Holman TJ, Jones PD, Russell L, Medhurst A, Ubeda TS, Talloji P, Marquez J, Schmuths H, Tung SA, Taylor I, et al. The N-end rule pathway promotes seed germination and establishment through removal of ABA sensitivity in Arabidopsis. Proc Natl Acad Sci USA 2009;106:4549–4554. [PubMed: 19255443]

Hu R-G, Sheng J, Xin Q, Xu Z, Takahashi TT, Varshavsky A. The N-end rule pathway as a nitric oxide sensor controlling the levels of multiple regulators. Nature 2005;437:981–986. [PubMed: 16222293]

Hu R-G, Wang H, Xia Z, Varshavsky A. The N-end rule pathway is a sensor of heme. Proc Natl Acad Sci USA 2008;105:76–81. [PubMed: 18162538]

Huang TT, Nijman SMB, Mirchandani KD, Galardy PJ, Cohn MA, Haas W, Gygi SP, Ploegh HP, Bernards R, D'Andrea AD. Regulation of monoubiquitinated PCNA by DUB autocleavage. Nat Cell Biol 2006;8:339–347. [PubMed: 16531995]

Hwang C-S, Shemorry A, Varshavsky A. Two proteolytic pathways regulate DNA repair by co-targeting the Mgt1 alkyguanine transferase. Proc Natl Acad Sci USA 2009;106:2142–2147. [PubMed: 19164530]

Hwang C-S, Varshavsky A. Regulation of peptide import through phosphorylation of Ubr1, the ubiquitin ligase of the N-end rule pathway. Proc Natl Acad Sci USA 2008;105:19188–19193. [PubMed: 19033468]

Johnson ES, Gonda DK, Varshavsky A. Cis-trans recognition and subunit-specific degradation of short-lived proteins. Nature 1990;346:287–291. [PubMed: 2165217]

Kwon YT, Balogh SA, Davydov IV, Kashina AS, Yoon JK, Xie Y, Gaur A, Hyde L, Denenberg VH, Varshavsky A. Altered activity, social behavior, and spatial memory in mice lacking the NTAN1 amidase and the asparagine branch of the N-end rule pathway. Mol Cell Biol 2000;20:4135–4148. [PubMed: 10805755]

Kwon YT, Kashina AS, Davydov IV, Hu R-G, An JY, Seo JW, Du F, Varshavsky A. An essential role of N-terminal arginylation in cardiovascular development. Science 2002;297:96–99. [PubMed: 12098698]

Lim J, Hao T, Shaw C, Patel AJ, Szabó G, Rual J-F, Fisk CJ, Li N, Smolyar A, Hill DE, et al. A protein-protein interaction network for human inherited ataxias and disorders of Purkinje cell degeneration. Cell 2006;125:801–814. [PubMed: 16713569]

Mogk A, Schmidt R, Bukau B. The N-end rule pathway of regulated proteolysis: prokaryotic and eukaryotic strategies. Trends Cell Biol 2007;17:165–172. [PubMed: 17306546]

Pedersen LC, Yee VC, Bishop PD, Le Trong I, Teller DC, Stenkamp RE. Transglutaminase factor XIII uses proteinase-like catalytic triad to crosslink macromolecules. Prot Sci 1994;3:1131–1135.

Prakash S, Inobe T, Hatch AJ, Matouschek A. Substrate selection by the proteasome during degradation of protein complexes. Nat Chem Biol 2009;5:29–36. [PubMed: 19029916]

Rao H, Uhlmann F, Nasmyth K, Varshavsky A. Degradation of a cohesin subunit by the N-end rule pathway is essential for chromosome stability. Nature 2001;410:955–960. [PubMed: 11309624]

Ravid T, Hochstrasser M. Diversity of degradation signals in the ubiquitin-proteasome system. Nat Rev Mol Cell Biol 2008;9:679–689. [PubMed: 18698327]

Schilling S, Wasternack C, Demuth HU. Glutaminyl cyclases from animal and plants: a case of functionally convergent evolution. Biol Chem 2008;389:983–991. [PubMed: 18979624]

Suzuki T, Varshavsky A. Degradation signals in the lysine-asparagine sequence space. EMBO J 1999;18:6017–6026. [PubMed: 10545113]

Tasaki T, Kwon YT. The mammalian N-end rule pathway: new insights into its components and physiological roles. Trends Biochem Sci 2007;32:520–528. [PubMed: 17962019]

Tasaki T, Zakrzewska A, Dudgeon D, Jiang Y, Lazo JS, Kwon YT. The substrate recognition domains of the N-end rule pathway. J Biol Chem 2009;284:1884–1895. [PubMed: 19008229]

Tian L, Wang P, Guo J, Wang X, Deng W, Zhang C, Fu D, Gao X, Shi T, Ma D. Screening for novel human genes associated with CRE pathway activation with cell microarray. Genomics 2007;90:28–34. [PubMed: 17490851]

Varshavsky A. The N-end rule: functions, mysteries, uses. Proc Natl Acad Sci USA 1996;93:12142–12149. [PubMed: 8901547]

Varshavsky A. Spalog and sequelog: neutral terms for spatial and sequence similarity. Curr Biol 2004;14:R181–R183. [PubMed: 15028230]

Varshavsky A. Ubiquitin fusion technique and related methods. Meth Enzymol 2005;399:777–799. [PubMed: 16338395]

Varshavsky A. Discovery of cellular regulation by protein degradation. J Biol Chem 2008a;283:34469–34489. [PubMed: 18708349]

Varshavsky A. The N-end rule at atomic resolution. Nat Struct Mol Biol 2008b;15:1238–1240. [PubMed: 19050717]

Wang KH, Roman-Hernandez G, Grant RA, Sauer TT, Baker TA. The molecular basis of N-end rule recognition. Mol Cell 2008;32:406–414. [PubMed: 18995838]

Xia Z, Turner GC, Hwang C-S, Byrd C, Varshavsky A. Amino acids induce peptide uptake via accelerated degradation of CUP9, the transcriptional repressor of the PTR2 peptide transporter. J Biol Chem 2008a;283:28958–28968. [PubMed: 18708352]

Xia Z, Webster A, Du F, Piatkov K, Ghislain M, Varshavsky A. Substrate-binding sites of UBR1, the ubiquitin ligase of the N-end rule pathway. J Biol Chem 2008b;283:24011–24028. [PubMed: 18566452]

Zenker M, Mayerle J, Lerch MM, Tagariello A, Zerres K, Durie PR, Beier M, Hülskamp G, Guzman C, Rehder H, et al. Deficiency of UBR1, a ubiquitin ligase of the N-end rule pathway, causes pancreatic

dysfunction, malformations and mental retardation (Johanson-Blizzard syndrome). Nat Genet 2005;37:1345–1350. [PubMed: 16311597]

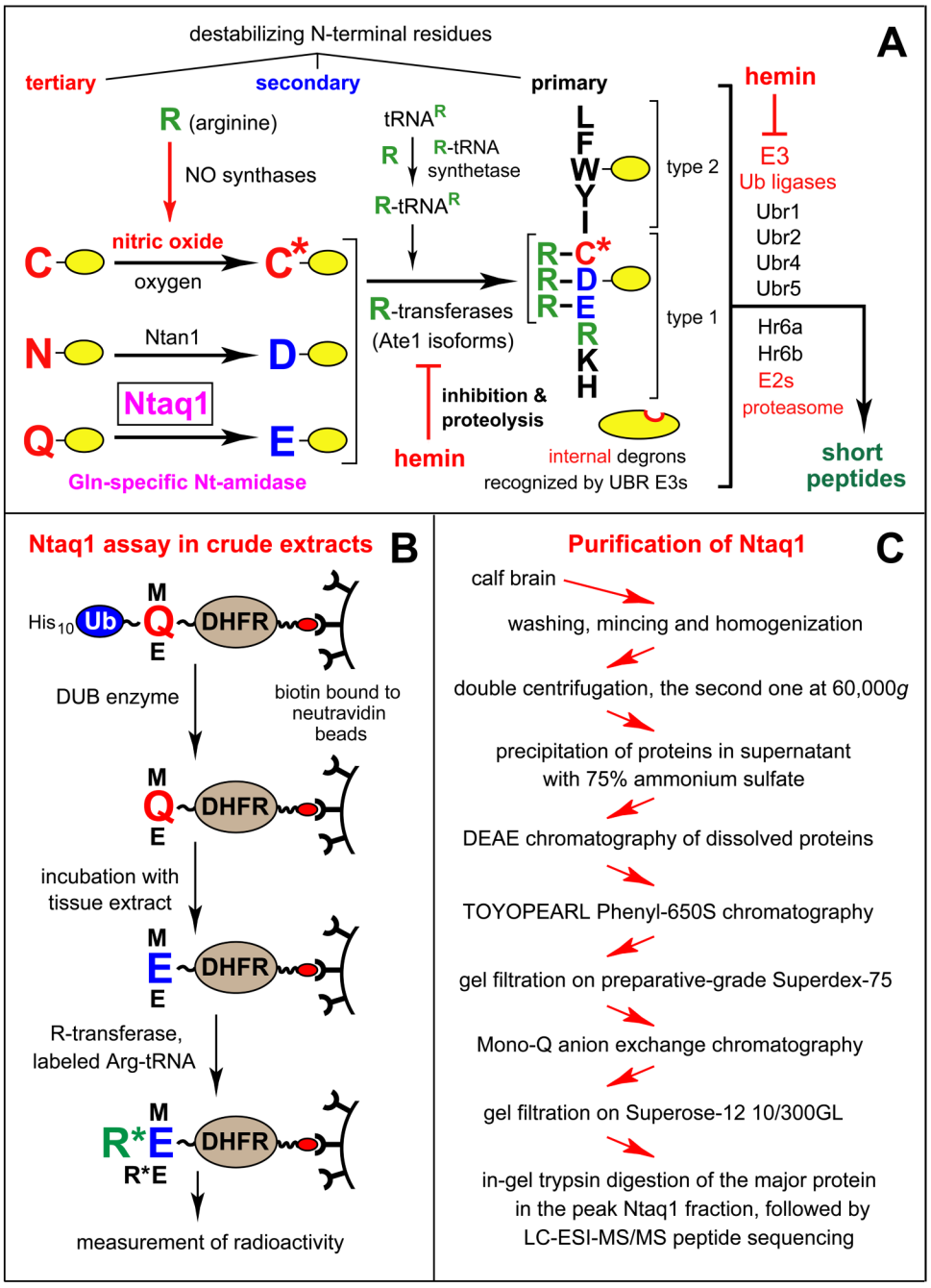

Figure 1. The Ntaq1 Nt^{Q}-amidase, a Component of the N-End Rule Pathway

(A) The mammalian N-end rule pathway. N-terminal residues are indicated by single-letter abbreviations for amino acids. Yellow ovals denote the rest of a protein substrate. “Primary”, “secondary” and “tertiary” denote mechanistically distinct subsets of destabilizing N-terminal residues (see Introduction). C* denotes oxidized Cys, either Cys-sulfinate or Cys-sulfonate. The enlarged and boxed “Ntaq1” term on the lower left denotes Nt^{Q}-amidase (amidohydrolase specific for N-terminal Gln) that was identified, isolated and characterized in the present work.

(B) Nt^{Q}-amidase assay.

(C) Purification of the bovine Ntaq1 Nt^{Q}-amidase (a condensed summary).

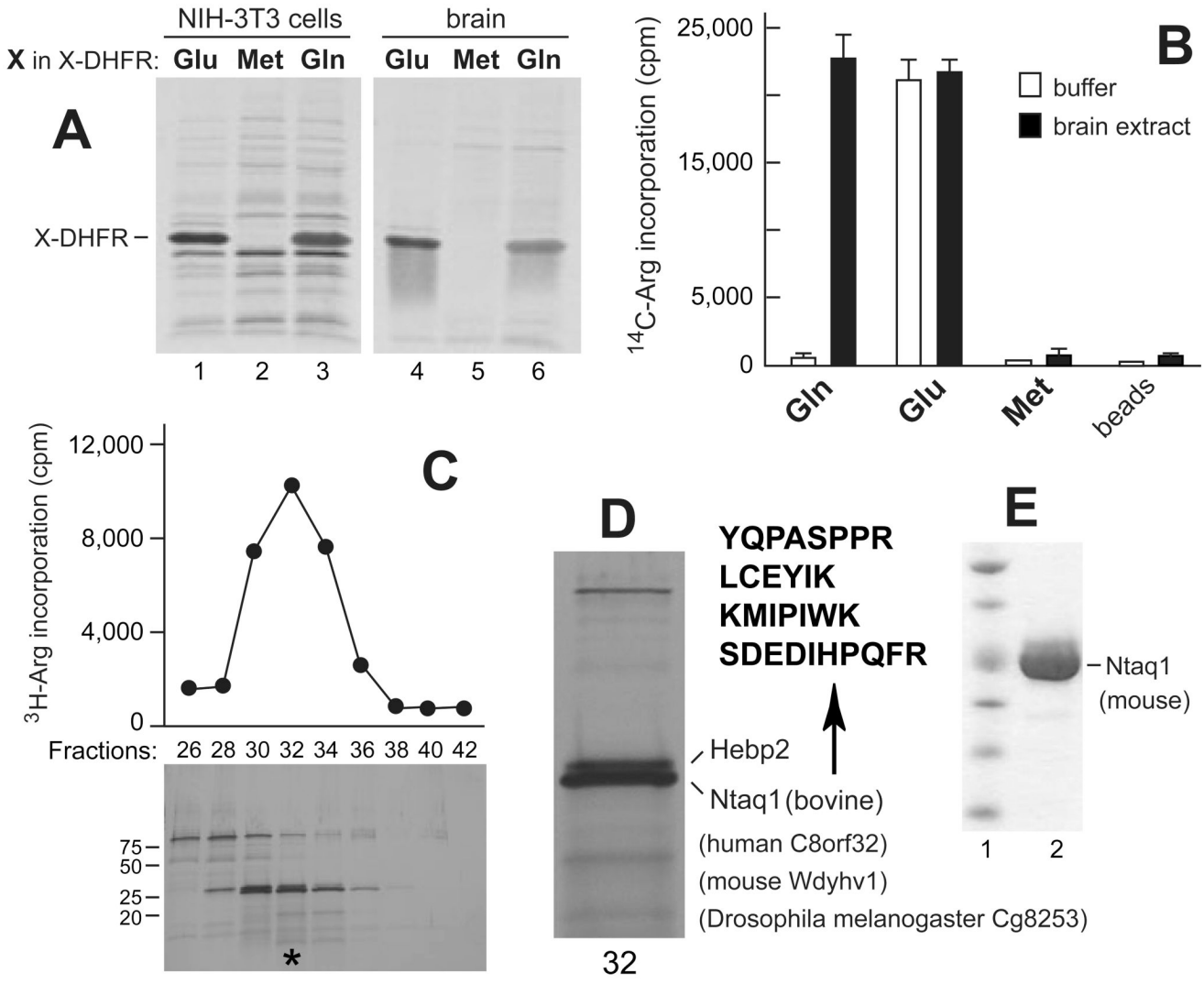

Figure 2. Detection and Purification of Ntaq1 Nt^Q-amidase

(A) Detection of the mouse Nt^Q-amidase activity in cell extracts. Lane 1, SDS-PAGE of ^{14}C-arginylated proteins in an extract of mouse NIH-3T3 cells containing the added Glu-DHFRbt reporter and processed as described in Figure 1B. Bands of ^{14}C-labeled X-DHFR reporters are indicated on the left. Lane 2, same as lane 1 but with Met-DHFRbt. Lane 3, same as lane 1 but with Gln-DHFRbt. Lanes 4–6, same as lanes 1–3 but with mouse brain extract.

(B) ^{14}C-arginylation assays with mouse brain extract or, alternatively, with buffer alone. These assays were similar to the one in lanes 4–6 of panel A, but with measurements of protein-conjugated ^{14}C-Arg. As shown here, the arginylation of Gln-DHFRbt required a preincubation with brain extract, whereas the arginylation of Glu-DHFRbt did not. A beads-alone control involved incubations of brain extract or buffer alone with beads lacking a bound reporter protein. Standard deviations, for duplicate measurements, are indicated above the bars.

(C) The last step of purification of bovine Ntaq1 Nt^Q-amidase, a gel filtration on Superose-12. Only fractions near the Ntaq1 activity peak (assayed as described in Figure 1B) are shown. Positions of M_r markers are indicated on the right of the SDS-PAGE pattern (silver staining). The asterisk denotes fraction 32, the peak activity fraction.

(D) Enlarged image of silver-stained proteins in fraction 32 of panel C. The identities of bovine Hebp2 and Ntaq1 were determined by mass spectrometry. A vertical arrow points to the

sequences of specific peptides of bovine Ntaq1 that were identified this way (Hebp2 peptides are not shown). The names of Genbank entries, in several organisms, for a protein that has now been identified (and named) as Ntaq1 are also shown.

(E) Coomassie-stained M_r markers (lane 1) and the C-terminally His_6-tagged mouse Ntaq1 Nt^Q-amidase (lane 2) that was purified from the yeast Pichia pastoris that overexpressed Ntaq1.

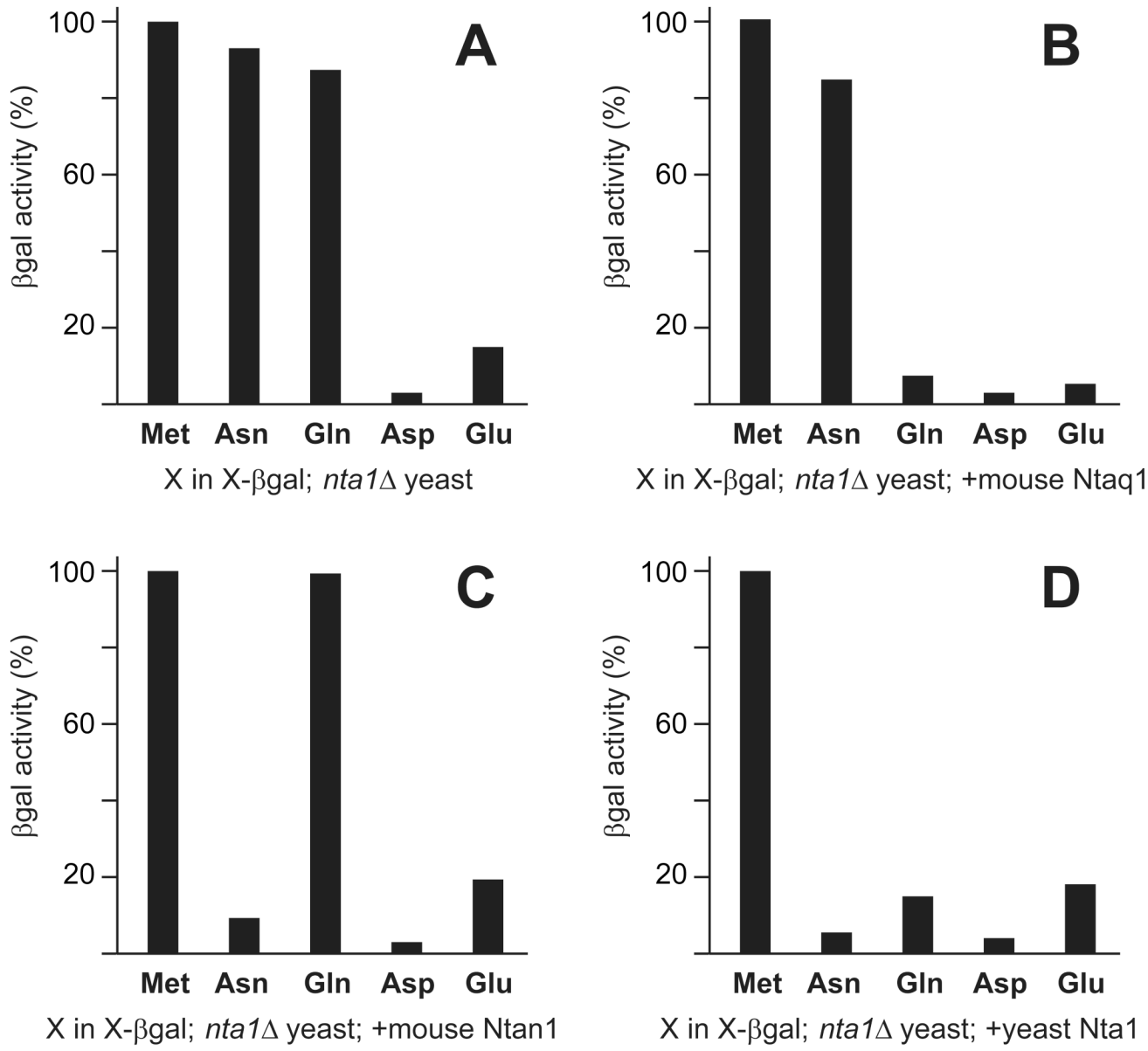

Figure 3. In Vivo Assays of Mouse Ntaq1 in the Yeast S. cerevisiae

(A) Measurements of βgal activity in extracts of S. cerevisiae that expressed X-βgal reporters bearing the indicated N-terminal residues were used to compare the metabolic stabilities of these reporters in an *nta1*Δ S. cerevisiae strain that also carried plasmids expressing specific Nt-amidases. 100% corresponds to the mean activity of βgal in extracts from cells expressing Met-βgal (Ub-Met-βgal), separately for each set of X-βgal assays in A–D. Results are averages of 3 independent measurements, which differed by less than 10% of the mean value.

(B) Same as in A but in the presence of mouse Ntaq1.

(C) Same as in A but in the presence of mouse Ntan1.

(D) Same as in A but in the presence of S. cerevisiae Nta1.

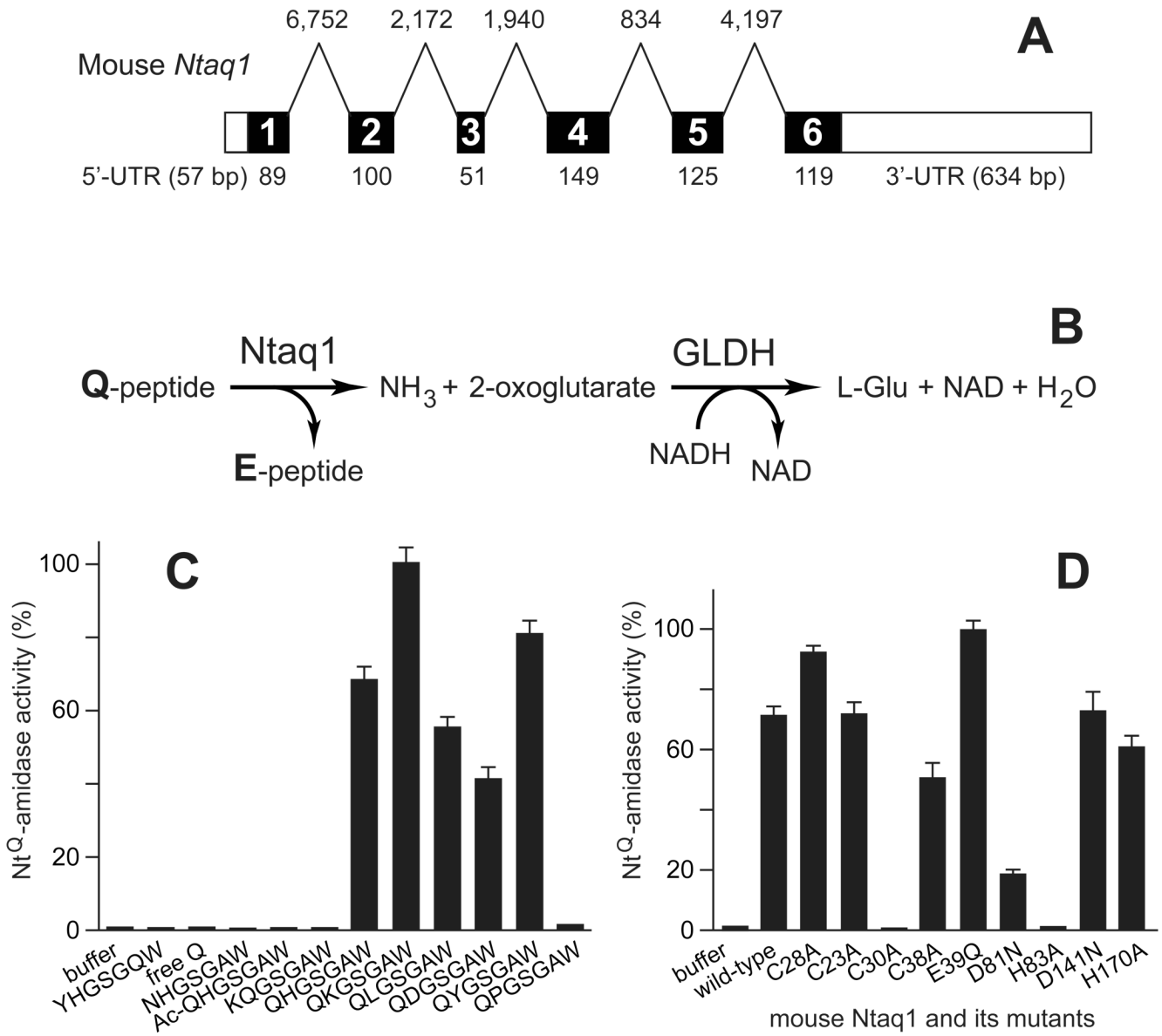

Figure 4. The Mouse *Ntaq1* Gene, the Specificity of Nt^{Q}-amidase, and Its Mutational Analysis

(A) The inferred structure of a mouse gene (Acc. No. NC_000081.5), termed *Ntaq1* in the present work, that encodes Nt^{Q}-amidase (see the main text). The inferred 3' and 5' untranslated regions (UTRs) of exons 1 and 6, respectively, are indicated by open rectangles. The inferred coding regions are in black. Their sizes, in bp, and the sizes of introns between them are also indicated.

(B) The Q-peptide assay for Nt^{Q}-amidase activity. In this coupled enzymatic assay, deamidation of N-terminal Gln is measured through utilization of released ammonia (NH_3) by NADH-dependent glutamate dehydrogenase (GLDH). The NH_3-dependent conversion, by GLDH, of NADH to NAD was monitored spectroscopically (see Supplemental Data).

(C) Activity of purified wild-type mouse Ntaq1 Nt^{Q}-amidase with test peptides. The Q-peptide assay was applied to a set of indicated 7-mer peptides. The activity of Ntaq1 with **Q**-KGSGAW was taken as 100%. It corresponded to 1.32 ± 0.11 nmole of **Q**-KGSGAW deamidated per second per nmole of Ntaq1.

(D) Comparisons of Nt^{Q}-amidase activity among wild-type Ntaq1 and its mutants. Measurements were carried out using the Q-peptide assay and **Q**-KGSGAW. The activity of $Ntaq1^{E39Q}$ (it exceeded the activity of wild-type Ntaq1) was taken as 100% in this set of tests. That activity corresponded to 1.49 ± 0.05 nmole of peptide deamidated per second per nmole of Ntaq1. Standard deviations, for triplicate measurements, are indicated above the bars in C and D.

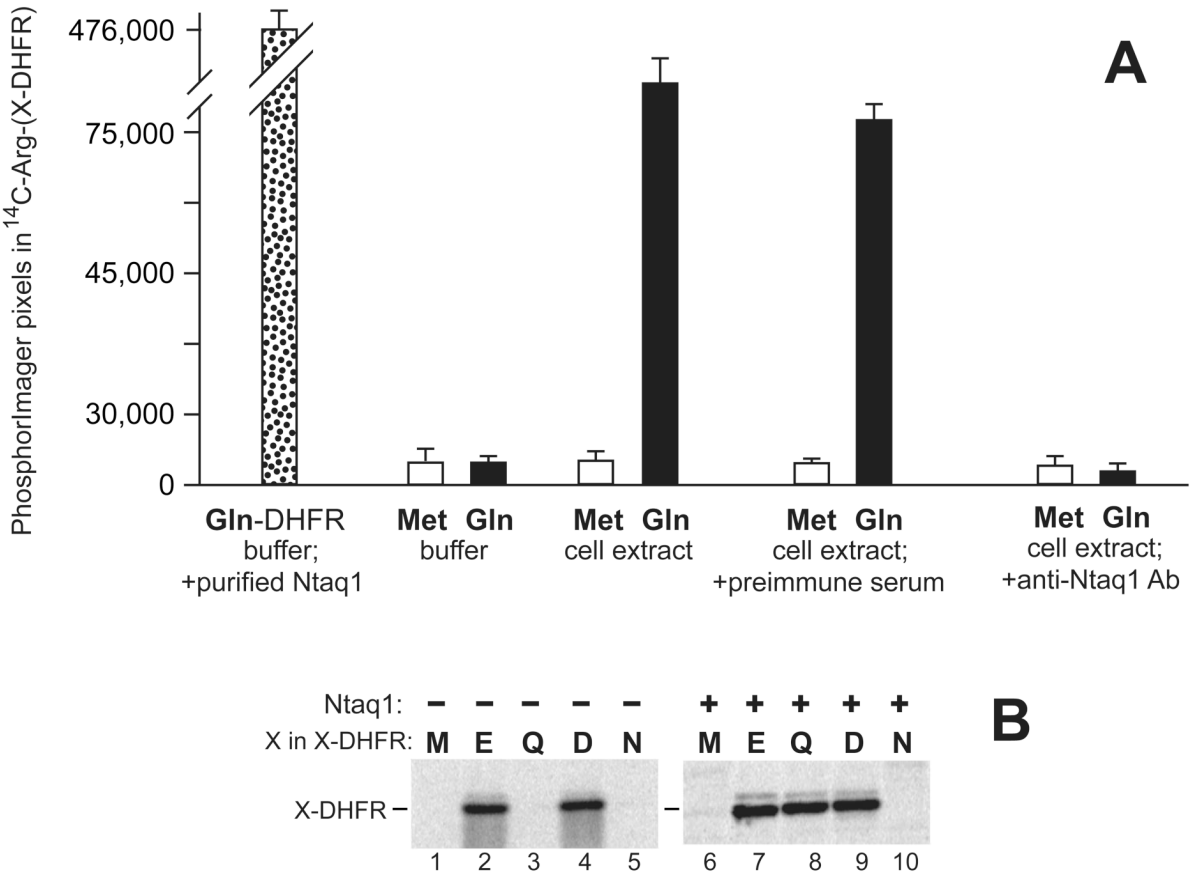

Figure 5. Substrate Specificity of the Ntaq1 Nt^{Q}-amidase and Antibody-Mediated Depletion of Ntaq1

(A) Depletion of Nt^{Q}-amidase activity from extracts of mouse NIH-3T3 cells by affinity-purified antibody to mouse Ntaq1. Met-DHFRbt (white bars; this reporter cannot be arginylated) or Gln-DHFRbt (black bars; this reporter can be arginylated after its N-terminal deamidation) were incubated with buffer alone; or with an extract from 3T3 cells; or with the same extract that had been depleted with preimmune serum; or with the same extract that had been depleted with anti-Ntaq1 antibody. ^{14}C-arginylation assay with purified R-transferase (Figure 1B) was carried out after these treatments, followed by SDS-PAGE and autoradiographic quantitation of a ^{14}C-arginylated reporter band, using PhosphorImager. A

dotted bar on the left shows the result of adding purified Ntaq1 (instead of buffer alone) to Gln-DHFRbt, followed by ^{14}C-arginylation. The much higher yield, in this test with purified Ntaq1, of Arg-Glu-DHFRbt implied that the bulk of Gln-DHFRbt remained non-deamidated by endogenous levels of the Ntaq1 Nt^{Q}-amidase in 3T3 cell extracts. Standard deviations, for duplicate measurements, are indicated above the bars.

(B) ^{14}C-arginylation assays (see Figure 1B), with **X**-DHFRbt reporters (**X** = M; E; Q; D; N) and the mouse Ntaq1 Nt^{Q}-amidase purified from P. pastoris (see Figure 2E). Lanes 1–5, the arginylation assay was carried out without preincubation with Ntaq1. Lanes 6–10, same as lanes 1–5 but the reporters were incubated with purified mouse Ntaq1 before ^{14}C-arginylation.

(C) N-terminal sequencing, by Edman degradation, of the indicated **X**-DHFRbt reporters (**X** = Q; N; E; MQ; GQ; EQ) after their incubation with purified mouse Ntaq1. N-terminal Glu, the result of Ntaq1-mediated deamidation of N-terminal Gln, is boxed in the middle row.

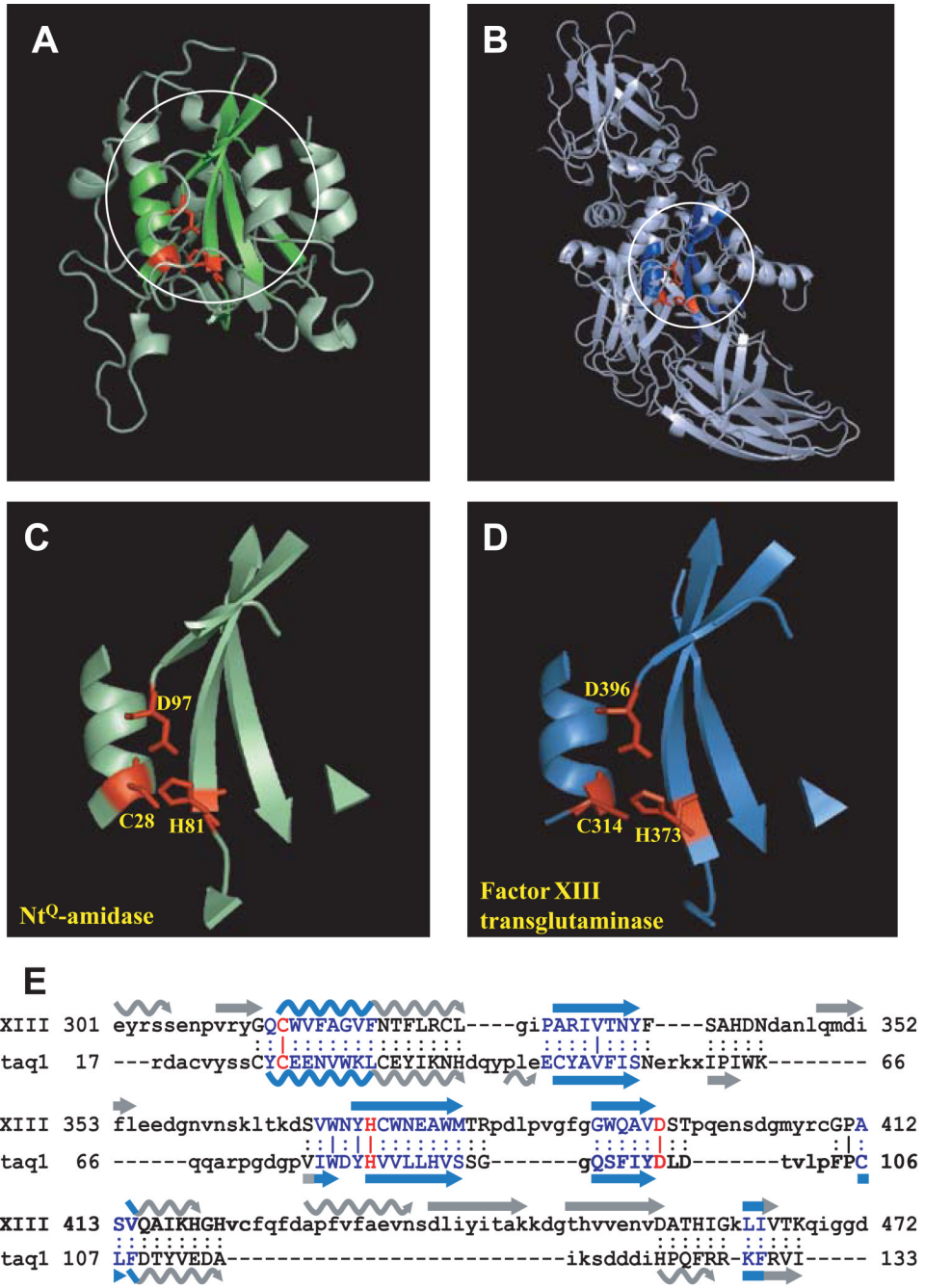

Figure 6. Structural Comparison of the Ntaq1 Nt^{Q}-amidase and Factor XIII Transglutaminase

(A and B) Crystal structures of the human Ntaq1 (C8orf32) Nt^{Q}-amidase (PDB 3C9Q) (Bitto et al., 2008) and FXIII transglutaminase (PDB 1FIE) (Pedersen et al., 1994), respectively. C8orf32, a previously uncharacterized human protein the structure of which was deposited in the Protein Data Bank (PDB 3C9Q) by the Center for Eukaryotic Structural Genomics (Bitto et al., 2008), was shown, in the present work, to be the Ntaq1 Nt^{Q}-amidase.

(C and D) Structures around the active sites of Ntaq1 Nt^{Q}-amidase and Factor XIII transglutaminase, respectively (these regions are circled in A and B). The catalytic triad of Factor XIII transglutaminase (Cys^{314}, His^{373}, and Asp^{396}) (panel D) (Pedersen et al., 1994) and the corresponding residues of human Ntaq1 (Cys^{28}, His^{81}, and Asp^{97}) (panel C) are

indicated. Despite the striking (shown) spalogy between these regions of two enzymes, there is no significant sequelogy between them.

(E) Structure-based sequence alignment of the human Ntaq1 Nt^{Q}-amidase (hNtaq1) and human Factor XIII transglutaminase (FXIII). Aligned and nonaligned residues are indicated by uppercase and lowercase letters, respectively. "-" indicates gaps in the alignment. Straight and wavy arrows denote β-strands and α-helices, respectively. Regions in blue correspond to aspects of active sites of these enzymes that are shown in red in A–D. See Supplemental Data for additional details.